Polymer 155 (2018) 89–98

Contents lists available at ScienceDirect

Polymer

journal homepage: www.elsevier.com/locate/polymer

Poly(ethylene 2,5-furandicarboxylate-mb-poly(tetramethylene glycol)) multiblock copolymers: From high tough thermoplastics to elastomers

Hongzhou Xie[a], Linbo Wu[a,*], Bo-Geng Li[a], Philippe Dubois[b,**]

[a] State Key Laboratory of Chemical Engineering at ZJU, Key Laboratory of Biomass Chemical Engineering of Ministry of Education, College of Chemical and Biological Engineering, Zhejiang University, Hangzhou, 310027, China

[b] Laboratory of Polymeric and Composite Materials (LPCM), Center of Innovation and Research in Materials and Polymers (CIRMAP), University of Mons, Mons, 7000, Belgium

HIGHLIGHTS

- P(EF-mb-PTMG) copolymers with high intrinsic viscosity have been synthesized.
- The PTMG segment is partially miscible with PEF and can slightly plasticize PEF.
- PEF-based materials can be tailor-made from high tough thermoplastics to elastomers.
- The presence of PTMG greatly improves toughness while keeping high strength of PEF.
- Supertough (> 50 kJ/m^2) PEF-based materials are reported for the first time.

ARTICLE INFO

Keywords:
poly(ethylene 2,5-furandicarboxylate)
Toughening
Multiblock copolymers

ABSTRACT

Poly(ethylene 2,5-furandicarboxylate) (PEF) is a biobased polyester with superior thermo-mechanical and gas barrier properties than poly(ethylene terephthalate) (PET), the most widely used petroleum-based polyester. However, PEF is more brittle than PET. To toughen PEF, a series of P(EF-mb-PTMG) (PETF) multiblock copolymers with high intrinsic viscosity were successfully synthesized via melt polycondensation in the presence of poly(tetramethylene glycol) (PTMG) oligomer diols, and characterized with FTIR, ^{1}H NMR, DSC, WAXD, TGA and SEM, and assessed with tensile and impact testing. The presence of PTMG contributes to promote intrinsic viscosity growth and depress etherification and discoloration side reactions. The PTMG flexible segments show chain length dependent partial miscibility with PEF hard segments, and its presence also plasticizes and promotes cold crystallization of PEF segments. With tuning the PTMG content, high performance PEF-based materials can be tailor-made from high tough thermoplastics with excellent ductility and impact toughness to thermoplastic elastomers with high strength. Particularly, PET^{1K}F-20 shows excellent ductility (elongation at break 252%) while retaining high modulus (3.0 GPa) and yielding strength (74 MPa), and PET^{1K}F-35 is the first PEF-based material with impact strength over 50 kJ/m^2 to date.

1. Introduction

Nowadays, the excessive utilization and discarding of polymeric materials based on petroleum resources have caused growing concerns about depletion of nonrenewable resources and environmental pollution [1–4]. As a typical instance, poly(ethylene terephthalate) (PET) has been produced at huge scale (over 50 million metric tons per year) and becomes the polyester most widely used in fibers, bottles, films and packaging materials in the past decades due to its optical clarity, barrier properties, tensile properties and competitive performance-to-cost ratio [5]. Although PET can be recycled to some extent, however, it inevitably becomes one of the major resources of polymer wastes [6]. On the other hand, relatively high oxygen and carbon dioxide permeability of PET limits its applications in gas-sensitive packages for food and beverage.

2,5-furandicarboxylic acid (FDCA) is a diacid monomer with rigid aromatic ring originated from biomass such as starch, cellulose or hemicellulose [7]. It has physical and chemical properties similar to the

* Corresponding author.
** Corresponding author.
E-mail addresses: wulinbohz@gmail.com (L. Wu), philippe.dubois@umons.ac.be (P. Dubois).

https://doi.org/10.1016/j.polymer.2018.09.033
Received 23 June 2018; Received in revised form 10 September 2018; Accepted 17 September 2018
Available online 19 September 2018

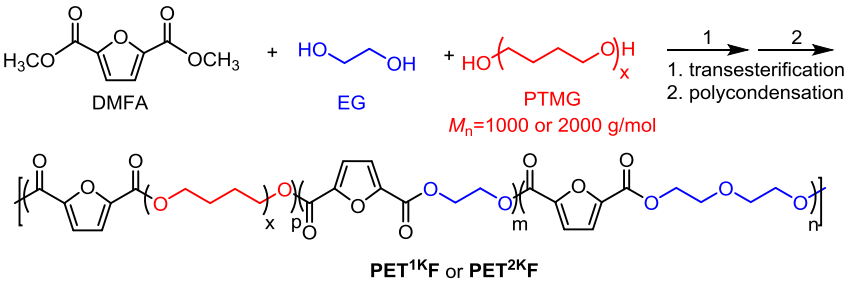

Scheme 1. Schematic diagram of synthesis of P(EF-mb-PTMG) (in abbr., PETF) copolymers.

petro-based monomer terephthalate acid (TPA). Polyesters synthesized from FDCA and various diols have attracted extensive attention in the last decade due to the biobased nature and possibly better properties or higher performance [8–15]. Among them, a lot of attention has been paid to poly(ethylene 2,5-furandicarboxylate) (PEF), a fully biobased polyester synthesized from FDCA or its diester and ethylene glycol (EG). In comparison with PET, it has not only higher glass transition temperature, higher tensile strength and modulus and lower melt processing temperature, but also about one order higher oxygen [16] and carbon dioxide [17] barrier performance as well as reduced environmental impacts during production [18]. These features make PEF a perfect biobased substitute of PET for high-demanding application, especially for high gas barrier applications.

However, PEF has inherent shortcomings, which limits its processing and applications, including very slow melt crystallization rate [10,19] and brittleness [20–23]. PEF shows poor ductility and impact toughness, which may result from its chain stiffness [28]. According to previous reports, it is more brittle than PET, showing elongation at break ranging 1–5% [15,20–27] and notched Izod impact strength around 3.1 kg cm/cm [20]. In order to obtain PEF materials with satisfactory performance, physical and chemical modifications of PEF, including nanocomposite [29,30], blending [31–33], random [20,21,24–26,34–37] and block [26] copolymerization have been frequently reported in the recent literature.

Terzopoulou et al. [35] and Ma et al. [37] reported the synthesis and properties of random copolyesters of PEF containing short chain diacid or diol unit, namely succinic acid and butanediol, but did not report the mechanical properties. Wang et al. [24] reported poly (ethylene sebacate-co-2,5-furandicarboxylate) (PESeF) as a random copolyester containing flexible sebacate units, but the modulus and strength decreased remarkably at low sebacate content and the elongation at break was not improved until high sebacate content (70 mol %) was used. In contrast, random copolyesters of PEF containing rigid units such as terephthalate [27], 1,4-cyclohexylene dimethylene [20,21] or 2,2,4,4-tetramethyl-1,3-cyclobutanediol [25] showed much higher modulus and strength, but the ductility was not improved until high content of comonomer, too. For an example, the elongation at break of poly(ethylene-co-1,4-cyclohexylene dimethylene 2,5-furandicarboxylate) (PECF) can be raised from 5% of PEF to 186% at 59 mol% CF unit, but only to 50% at 32 mol% CF unit [21]. Wang et al. [26] synthesized P(EF-mb-PEG) multiblock copolymers containing poly (ethylene glycol) (PEG) soft segments. The strength decreased to 27 MPa at 20 w% PEG content, but the elongation at break was slightly raised to 35% up to 60 w% PEG. The improvement of PEF ductility seems to be limited. For improving impact toughness of PEF, Park et al. [20] reported the first and sole result to date. They found the impact strength of PECF can be slightly improved with respect to PEF, from 3.1 kg cm/cm of PEF to 4.0 kg cm/cm of $PE_{25}C_{75}F$. Clearly, the improvement is also very limited.

In order to improve ductility and impact toughness of PEF and obtain PEF-based materials with balanced mechanical performance, in this study, PEF-based multiblock copolymers, namely, poly(ethylene 2,5-furandicarboxylate-mb-poly(tetramethylene glycol) (P(EF-mb-PTMG), or PETF for simplicity) were synthesized via melt polycondensation of dimethyl 2,5-furandicarboxylate (DMFD) and ethylene glycol (EG) in presence of PTMG diols. Chain structure and composition of the products were characterized with FTIR and ^{1}H NMR, and crystallization, fracture morphology and thermo-mechanical properties were assessed with DSC, XRD, TGA, SEM, tensile and notched Izod impact testing. The effect of chain length and content of PTMG on the structure and properties have been discussed. It is worth pointing out that PTMG is potentially biobased as well and has been employed as a precursor in synthesizing other poly(ether-ester) segmented copolymers including P(BT-mb-PTMG)s as the well-known commercial polyester elastomers [38,39] and P(BF-mb-PTMG)s as modified PBF materials [40]. However, to our best knowledge, synthesis and properties of P(EF-mb-PTMG)s have not been reported yet.

2. Experimental part

2.1. Materials

Dimethyl 2,5-furandicarboxylate (DMFD, 99.3% according to the supplier) was a product from Mianyang ChemTarget. Co. Ltd, China. Ethylene glycol (EG, 99%, Sigma), poly(tetramethylene glycol) (PTMG, $M_n \approx$ 1000, 2000 g/mol, Macklin) and Irganox 1010 (BASF) were used without any further purification. Home-made titanium-silica complex (Ti@Si, Ti 1 w% or 0.21 mmol Ti/g) was used as the catalyst for polymer synthesis. Phenol, 1,1,2,2-tetrachloroethane (TCE), acetone, ethanol, deuterated chloroform ($CDCl_3$) and deuterated trifluoroacetic acid (TFA-d_1) were all purchased from Sinopharm and used as received.

2.2. Synthesis of PEF and P(EF-mb-PTMG) (or PETF) copolymers

The PEF and P(EF-mb-PTMG) copolymers were synthesized from DMFD, EG, and PTMG via a two-stage melt polycondensation method (Scheme 1). The molar ratio EG/DMFD was fixed at 2, but the PTMG/EG mass ratio changed and ranged from 0 to 3.43. In the first step, the calculated amounts of DMFD, EG, PTMG, thermal stabilizer (Irganox 1010, 0.25 w% based on the total monomer mass), and catalyst (0.1 w % based on DMFD) were charged into a 250 mL four-necked round-bottom reactor equipped with a mechanical stirrer, N_2 inlet and reflux condenser. Then, the transesterification reaction was carried out at 170–200 °C for about 4 h under the protection of N_2 until there was no methanol, the byproduct, to be distilled out. In the second step, the reaction temperature was increased to 230–240 °C for polycondonsation reaction under a reduced pressure of about 100 Pa. The reaction was stopped when a so-called Weissenberg effect emerged. Finally, the products ware dried at 60 °C in vacuum for characterization.

For simplicity, the resulting multiblock copolymers, P(EF-mb-PTMG)s, are named as PETF, or more precisely, PET^{x}F-y, where x indicates the number-average molecular weight of PTMG (1K and 2K represent 1000 g/mol and 2000 g/mol, respectively) and y indicates the expected mass percentage of PTMG (φ_{PTMG}) to be fully incorporated into the copolymers, which is calculated according to equation (1). In the equation, m_{PTMG} and m_{DMFD} are the mass of PTMG and DMFD in

Table 1
Molecular characteristics and decomposition temperature of PEF and PETF copolymers.

Sample	φ_{PTMG}[a] (w%)	^{1}H NMR				[η][f] (dL/g)	$T_{d,5}$[g] (°C)	$T_{d,max}$[g] (°C)
		ϕ_{PTMG}[b] (w%)	ϕ_{DEGF}[c] (mol%)	$X_{n,PEF}$[d]	$M_{n,PEF}$[e] (g/mol)			
PEF	0	0	2.31	–	–	0.81	376	416
PET^{1K}F-10	10	9.5	2.39	46.2	8400	0.83	337	391
PET^{1K}F-20	20	19.7	2.18	19.4	3540	1.13	333	390
PET^{1K}F-30	30	29.7	1.69	12.2	2210	0.97	334	386
PET^{1K}F-40	40	40.4	1.44	7.1	1280	1.03	335	387
PET^{1K}F-50	50	50.9	1.16	6.4	1160	0.98	338	388
PET^{1K}F-60	60	61.2	1.01	4.6	841	1.23	341	391
PET^{1K}F-70	70	75.6	0.72	1.6	284	1.41	342	394
PET^{2K}F-10	10	9.4	3.82	45.2	8220	0.75	nd	nd
PET^{2K}F-20	20	19.7	2.13	19.3	3500	0.97	nd	nd
PET^{2K}F-30	30	29.8	1.88	13.9	2530	1.14	nd	nd

[a] Expected mass percentage of PTMG prepolymer in feed, calculated with equation (1).
[b] Mass percentage of PTMG segment in the copolymers, measured with ^{1}H NMR and calculated with equation (2).
[c] Molar percentage of DEGF repeat unit in the PEF segments, calculated with equation (3).
[d] Number-average polymerization degree of PEF segment calibrated with equation S3, $X_{n,PEF} = X'_{n,PEF}*12.4/X'_{n,PTMG}$.
[e] Number-average molecular weight of PEF segment calculated by $M_{n,PEF} = X_{n,PEF}*182$ g/mol.
[f] Intrinsic viscosity, measured at 25 °C using phenol/1,1,2,2- tetrachloroethane (3/2, w/w) mixture solvent.
[g] Characteristic temperatures at 5% and rapidest weight loss in TGA curves.

feed, and 182 and 184 are the molecular weights of the rigid repeat unit EF and monomer DMFD, respectively.

$$y = \varphi_{PTMG}(\%) = \frac{m_{PTMG}}{m_{PTMG} + \frac{182 m_{DMFD}}{184}} * 100\% \quad (1)$$

2.3. Characterizations

Intrinsic viscosity [η] of the polyesters was measured at 25 °C with a semiautomatic viscosity tester (ZONWON IVS300, China) equipped with a Ubbelohde viscometer, using a 5 g/dL polyester solution in a mixture of solvents, i.e., phenol/1,1,2,2- tetrachloroethane (3/2, w/w).

ATR-FTIR spectra of the polyesters were recorded with a Nicolet 5700 spectroscopy (Thermo Fisher Scientific, USA) equipped with a germanium crystal ATR accessory. Disc specimens were prepared by hot-press molding at 250 °C.

^{1}H NMR spectra of the polyesters were recorded on a Bruker AC-80 (400 M). Deuterated trifluoroacetic acid (d_1-TFA) was used as solvent and tetramethylsilane as internal reference.

Thermal transition of the polyesters was recorded with differential scanning calorimetry (DSC) on a TA-Q200 (TA Instrument, USA) thermal analyzer using the traditional heating-cooling-heating cycle. The same heating/cooling rate, 10 °C/min, and the same isothermal time, 5 min, were used for all samples. But the temperature range depended on the type of sample: −90–100 °C for PTMGs, 30–250 °C for PEF and −90–250 °C for PETFs.

Thermogravimetric analysis (TGA) of the polyesters was carried out with a TA Q500 (TA Instrument, USA). All the samples were measured under a nitrogen atmosphere with a heating rate of 10 °C/min from 50 to 650 °C.

Wide angle X-ray diffraction (WAXD) patterns of the polyesters were recorded on a PANalytical X'Pert X-ray diffraction system (PANalytical Company) with CuK_α radiation (1.54 Å), working at 40 KV and 40 mA. The sample was scanned from 2θ = 5° to 2θ = 40° with a step size of 0.026° and an acquisition time of 30 s per step.

Tensile properties of the polyesters were measured with a Zwick Roell Z020 (Zwick, Germany) testing machine at room temperature according to ASTM D638. The dumbbell-shaped specimens with 2 mm in thickness and 4 mm in width were prepared by a HAAKE MiniJet Injection moulding machine and then conditioned at room temperature and 50% relative humidity for at least 48 h before testing. A crosshead speed of 10 mm/min was adopted for PEF, PET^{1K}F-10 and PET^{2K}F-10, but 20 mm/min for other samples. For each sample, at least five specimens were tested.

Notched Izod impact of the polyesters was measured using a CEAST Resil impact tester (CEAST, Italy) with a pendulum of 5.5 J according to ASTM D256. Specimens with 80 mm in length, 10 mm in width and 4 mm in thickness were prepared by a HAAKE MiniJet Injection moulding machine. All specimens were notched and conditioned at room temperature for at least 48 h before testing. At least five specimens were tested for each sample.

The fracture morphology of the impact fracture surface of PEF, PET^{1K}F-30, PET^{2K}F-30 and PET^{1K}F-35 were observed with SU-3500 (HITACHI, Japan) scanning electron microscopy at an acceleration voltage of 30 kV. The impact fracture surface was coated with a thin golden layer before observation.

Oxygen permeability of the (co)polymers was measured at 23 °C and 50% of relative humidity by using Labthink PERME OX2/231 O_2 permeability tester based on isopiestic determination method using high purity oxygen at 1 atm. Film samples were prepared with a Laboratory Compression Press (Gotech GT-7014-A50C, Taiwan, China). Firstly, small pieces of samples were sandwiched and melt between two Teflon sheets at 250 °C for 10 min without any pressure. Then, a pressure of about 150 bar was applied for 5 min before immediately quenching to room temperature by cold water. The film thickness was controlled by the stainless steel sheet (200 μm thick) with a 10 cm × 10 cm hole cut for placing sample. All the prepared film samples were measured as about 200 μm by coating thickness gauge (Ruige, Shanghai, RG260). Three films were tested for each sample.

3. Results and discussion

3.1. Synthesis and structure characterization

Two series of PETF copolymers, namely, PET^{1K}F-y (y = 10–70) and PET^{2K}F-y (y = 10–30) were synthesized using PTMG1000 (PTMG^{1K}) and PTMG2000 (PTMG^{2K}) respectively as prepolymers of the soft segments. All of the copolymers appear oyster white while the PEF homopolymer appears light amber. As shown in Table 1, the intrinsic viscosity ranges 0.75–1.41 dL/g and displays upward trend with increasing PTMG feeding though there is deviation in some data. The existence of PTMG seems to be helpful for molecular weight growth of the copolymers though the reason involved is not clear yet.

Chemical structure of the copolymers was determined by ATR-FTIR and ^{1}H NMR. Fig. 1 shows the FTIR spectra of PEF and PET^{1K}F copolymers. There appear typical absorption peaks of furan ring, including

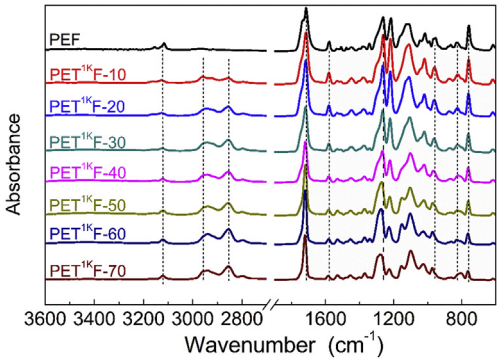

Fig. 1. ATR-FTIR of the PEF and PET^{1K}F copolymers.

the stretching vibration of C-H at 3123 cm^{-1}, the stretching vibration of C=C at 1580 cm^{-1}, ring breathing at 1022 cm^{-1} and ring bending at 969 cm^{-1}, 826 cm^{-1} and 761 cm^{-1}. The absorption peaks at 2939 cm^{-1} and 2855 cm^{-1} are attributed to the asymmetric and symmetric vibrations in C-H bonds of CH_2 group in PEF and PTMG segments. Notably, the intensity of the absorption peaks of furan ring decreases but that of CH_2 group increases when more PTMG is incorporated. In addition, the strong absorption peaks of C=O in ester bonds at 1714-1720 cm^{-1} and C-O in ester bonds at 1261-1278 cm^{-1} show blue shift with increasing the content of PTMG. These results indicate that the PTMG segments are successfully incorporated into the copolymer chains. In addition, the signal around 3400 cm^{-1} corresponding to the terminal hydroxyl groups is invisible, indicating high molecular weight of the synthesized copolymers.

As PEF and the PETF copolymers are insoluble in common deuterated solvents except deuterated trifluoroacetic acid (TFA-d_1) and hexafluoroisopropanol, ^{1}H NMR spectra of them were recorded using TFA-d_1 as solvent. Fig. 2 shows the ^{1}H NMR spectra of PEF and PET^{1K}F copolymers. For PEF, the chemical shifts of CH in furan ring and CH_2 in EG unit appear at 7.46 ppm (F) and 4.88 ppm (a), respectively. In addition, the chemical shifts of the outer and inner CH_2 in diethylene glycol furancarboxylate (DEGF) repeat unit which was formed via etherification side reaction [10] are presented at 4.76 ppm and 4.25 ppm, respectively. For the PET^{1K}F copolymers, in addition to the chemical shifts of EF and DEGF units in PEF segments, the chemical shifts of the outer CH_2 in PTMG segments adjacent to the ester bonds and ether bonds are observed at 4.03 ppm (b) and 3.81 ppm (e + f); and the chemical shifts of the inner CH_2 in PTMG appear at 2.08 ppm (c) and 1.82 ppm (d + g), respectively. The small but unexpected chemical shifts at 4.55 ppm and 1.95 ppm are identified as chemical shifts from the products possibly formed via TFA-d_1-catalyzed

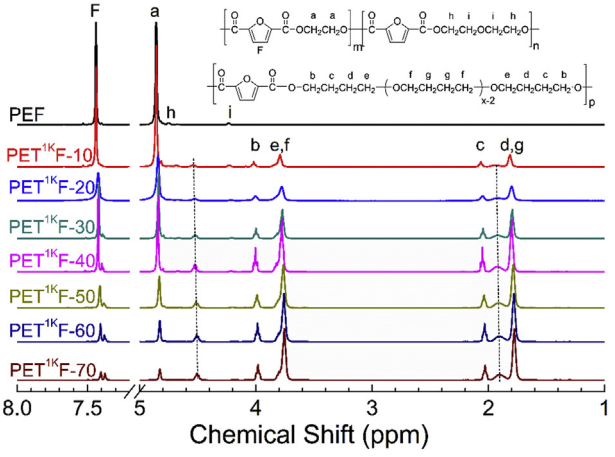

Fig. 2. ^{1}H NMR spectra of PEF and PET^{1K}F copolymers.

decomposition of PTMG segment. Detailed analyses are shown in the Supporting Information. For the PET^{2K}F copolymers, similar results are also obtained, as shown in Fig. S1. Therefore, the multiblock copolymers with expected chemical structure containing PTMG soft segments and PEF hard segments composed of EF (major) and DEGF (minor) repeat units (Scheme 1) have been successfully synthesized.

Because of the decomposition of PTMG segment in the presence of the ^{1}H NMR solvent TFA-d_1, the number-average polymerization degrees or molecular weights ($X_n^{'}$ or $M_n^{'}$) of PEF and PTMG segments directly calculated from the ^{1}H NMR spectra are all underestimated (for details, see Supporting Information). But the true values can still be obtained through reasonable calibration (see Supporting Information) and the results are listed in Table 1. Fortunately, such decomposition does not affect the calculation of the weight percentage of PTMG soft segments in the copolymer (ϕ_{PTMG}) and the molar percentage of DEGF unit in PEF hard segments (ϕ_{DEGF}). They can be calculated from the ^{1}H NMR spectra using equations (2) and (3), respectively, where I_a, I_{e+f} and I_i are the abbreviations of the integral intensities of chemical shifts a, e + f and i, and 72, 182 and 226 are the molecular weights of TMG, EF and DEGF repeat units, respectively. From the result listed in Table 1, it can be seen that the weight percentages of PTMG in the copolymers measured from ^{1}H NMR (ϕ_{PTMG}) agree well with the expected values calculated from feeding (φ_{PTMG}) except for PET^{1K}F-70. The X_n of PEF segments ranges 46-2 and decreases with increasing ϕ_{PTMG} because the PEF chains are partitioned by PTMG to more segments. The ϕ_{DEGF} value is small (3.82–0.72 mol%) and decreases with increasing ϕ_{PTMG}. The results indicate that the existence of PTMG is very beneficial for the polycondensation reaction, not only promoting molecular weight growth, but also depressing the formation of DEGF unit. The reason is not clear yet and needs further study.

$$\phi_{PTMG}(w\%) = \frac{72(I_b + I_e + I_f)}{72(I_b + I_e + I_f) + 182I_a + 226I_i} * 100\% \quad (2)$$

$$\phi_{DEGF}(mol\%) = \frac{I_i}{I_i + I_a} * 100\% \quad (3)$$

3.2. Thermal transition behavior

The cooling and 2nd heating DSC thermograms of PTMG prepolymers, PEF and PETF copolymers are shown in Fig. 3. The thermal transition properties are summarized in Table 2 and their composition dependences are illustrated in Fig. 4. The PEF sample showed no melt crystallization peak in the cooling scan but a very weak melting peak with the enthalpy (ΔH_m) of 1.2 J/g at 213.4 °C in the 2nd heating scan, indicating that PEF is a semicrystalline polyester with very weak melt crystallizability. In the first heating scan, it exhibited a melting peak with ΔH_m of 10.7 J/g at 213.4 °C (Fig. S3 and Table S3). In contrast, the PTMGs are strong crystalline prepolymers. The PTMG^{1K} and PTMG^{2K} prepolymers showed rapid melt crystallization during cooling scan and intensive melting peaks in second heating, without observable glass transition and cold crystallization. In comparison, PTMG^{2K} crystallized a little more rapidly than PTMG^{1K}, showing higher melt crystallization temperature (T_c, 5.7 °C vs. 1.2 °C) and enthalpy (ΔH_c, 94.3 J/g vs. 88.5 J/g), and higher melting temperature (T_m, 26.3 °C vs. 21.7 °C) and enthalpy (ΔH_m, 101.5 J/g vs. 92.3 J/g).

In the PET^{1K}F copolymers, the PTMG^{1K} segment shows neither crystallization nor melting peak, suggesting that the PTMG^{1K} segment is strongly restrained in chain motion by the adjacent PEF segments and therefore losses its crystallizability. In comparison with PEF homopolymer, the PEF segment in PET^{1K}F does not show melt crystallization too, but exhibits clearly enhanced cold crystallization and melting peaks, indicating that the presence of PTMG segments promotes chain motion of the PEF segments and therefore cold crystallization occurs. For an example, the crystallinity increases from 0.9% of PEF homopolymer to 27% of PET^{1K}F-10 in the presence of only 10 w% PTMG^{1K}

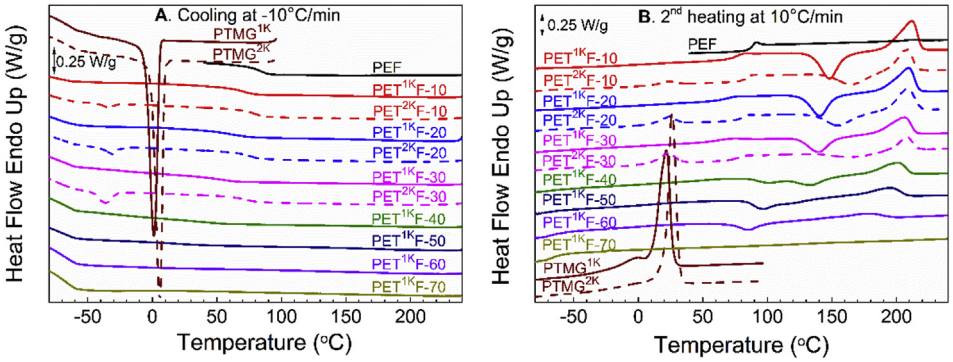

Fig. 3. DSC curves of PTMG1000 ($PTMG^{1K}$), PTMG2000 ($PTMG^{2K}$), PEF and PETF copolymers: A. cooling scan at −10 °C/min, B. 2nd heating scan at 10 °C/min.

segment. With increasing the weight percentage of $PTMG^{1K}$ segment (ϕ_{PTMG}), the PEF segments gain increasing chain mobility and therefore show decreasing T_{cc} accordingly. On the other hand, the sequence length of PEF segments decreases with increasing ϕ_{PTMG} (see Table 1), therefore, the crystallizability decreases and the ΔH_{cc}, ΔH_m as well as T_m all decreases accordingly. $PET^{1K}F$-70 no longer shows cold crystallization and melting because of too short chain length (X_n = 1.6, M_n = 284 g/mol). The crystallinity of PEF segment in $PET^{1K}F$ copolymers is measured in a rather narrow range between 23 and 28% at ϕ_{PTMG} of 10–60%, not showing clear ϕ_{PTMG} dependence.

In addition, the $PET^{1K}F$ copolymers show a single glass transition corresponding to PEF segments, which shifts to lower temperature and becomes weaker with increasing ϕ_{PTMG}, being invisible up to ϕ_{PTMG} of 70%. This result suggests that PEF and $PTMG^{1K}$ segments display some extent of miscibility. However, it can be seen that the T_g data are clearly higher than the values calculated by the well-known Fox equation (Fig. 4A) in which two components of a copolymer are assumed to be completely miscible. Therefore, it can be concluded that in the $PET^{1K}F$ copolymers, the PEF rigid segments and $PTMG^{1K}$ flexible segments are partially miscible with each other, and therefore PEF segments are plasticized by $PTMG^{1K}$ to certain extent. Among these copolymers, $PET^{1K}F$-20 has a T_g of 68 °C, being lower the T_g of PEF (89 °C) but comparable to the T_g of PET (~75 °C).

In the $PET^{2K}F$ copolymers, the presence of $PTMG^{2K}$ segments also promotes the cold crystallization of PEF segment, therefore enhanced cold crystallization and melting peaks of PEF segments are observed too. But on the other hand, the $PET^{2K}Fs$ behave very differently from the $PET^{1K}F$ analogues. Firstly, melt crystallization and 2nd melting peaks of $PTMG^{2K}$ segments are observed, though the ΔH_c and ΔH_m are much smaller than those of the $PTMG^{2K}$ prepolymer. This means that although the crystallizability of $PTMG^{2K}$ is dramatically depressed, it still retains crystallizability to certain extent because of longer chain length, better chain mobility and therefore superior crystallizability than $PTMG^{1K}$ segments. Secondly, the $PET^{2K}F$ copolymers also show a single composition-dependent T_g, but the T_g shows weaker ϕ_{PTMG} dependence and therefore is clearly higher than that of $PET^{1K}F$ copolymers at the same ϕ_{PTMG} (see Fig. 4A). This result indicates that the miscibility between PEF and PTMG segments depends on PTMG chain length, so $PTMG^{2K}$ is still partially miscible with PEF segments, but less miscible when compared to $PTMG^{1K}$ counterpart. Because of the weaker miscibility with PEF segments, its promoting effect on crystallization of PEF segments is weaker than $PTMG^{1K}$ segment. For this reason, the $PET^{2K}F$ copolymers show higher T_{cc} and lower ΔH_{cc} and ΔH_m of PEF segments than $PET^{1K}Fs$ (see Fig. 4B).

3.3. Crystal structure

The WAXD patterns of PEF, $PET^{1K}F$-20, $PET^{1K}F$-40 and $PET^{1K}F$-60 were recorded after they were quenched from melt and cold crystallized at temperature close to T_{cc} (90 °C for $PET^{1K}F$-60 and 150 °C for others) for 3 h. The results are shown in Fig. 5. It is well known that the crystal structure of PEF is strongly influenced by the experimental conditions. Two kinds of crystal structure, named α-type crystal structure and α′-type crystal structure, can be obtained at high crystallization temperature (T_c > 170 °C) and low crystallization temperature (T_c < 170 °C) respectively [43]. In addition, β-type crystal structure can be formed by the solvent-induced crystallization [44]. Recently, the cell parameter of the above three crystal structure of PEF has been further studied by Maini et al. [45]. In this work, PEF shows strong reflections at 16.2°, 18.0°, 20.7°, 23.3° and 26.7° after crystallizing at

Table 2
Thermal transition properties of PTMG prepolymers, PEF and PETF copolymers.

Sample	Flexible PTMG segment					Rigid PEF segment					
	T_c (°C)	ΔH_c (J/g)	T_m (°C)	ΔH_m (J/g)	X_c[a] (%)	T_g (°C)	T_{cc} (°C)	ΔH_{cc} (J/g)	T_m (°C)	ΔH_m (J/g)	X_c[b] (%)
$PTMG^{1K}$	1.2	88.5	21.7	92.3	54	–	–	–	–	–	–
$PTMG^{2K}$	5.7	94.3	26.3	101.5	59	–	–	–	–	–	–
PEF	–	–	–	–	–	89	nd	nd	213.4	1.2	0.86
$PET^{1K}F$-10	nd	nd	nd	nd	nd	78	148.3	32.9	211.9	34.2	27
$PET^{1K}F$-20	nd	nd	nd	nd	nd	68	140.9	28	209.5	28.9	26
$PET^{1K}F$-30	nd	nd	nd	nd	nd	63	140.6	21.9	206.5	22.2	23
$PET^{1K}F$-40	nd	nd	nd	nd	nd	55	133.8	20.4	201.1	20.7	25
$PET^{1K}F$-50	nd	nd	nd	nd	nd	37	97.2	18.3	194.4	19.1	28
$PET^{1K}F$-60	nd	nd	nd	nd	nd	16	85.7	12	176.8	12.9	24
$PET^{1K}F$-70	nd	nd	nd	nd	nd	nd	nd	0	nd	0	0
$PET^{2K}F$-10	−34.9	3.2	23.5	3.4	21	85	165.8	21.1	207.4	21.1	17
$PET^{2K}F$-20	−31.4	6.4	23.2	6.8	20	82	155.5	23.2	208.8	23.8	21
$PET^{2K}F$-30	−37.7	10.5	23.2	11.7	23	79	163.6	11.2	208.5	11.8	12

[a] Crystallinity of PTMG segments calculated from $X_c = \Delta H_m/\phi_{PTMG}/\Delta H_{m0}$, where ΔH_{m0} (172 J/g) is melting enthalpy of completely crystallized PTMG [42].
[b] Crystallinity of PEF segments calculated from $X_c = \Delta H_m/(1\text{-}\phi_{PTMG})/\Delta H_{m0}$, where ΔH_{m0} (140 J/g) is melting enthalpy of completely crystallized PEF [10].

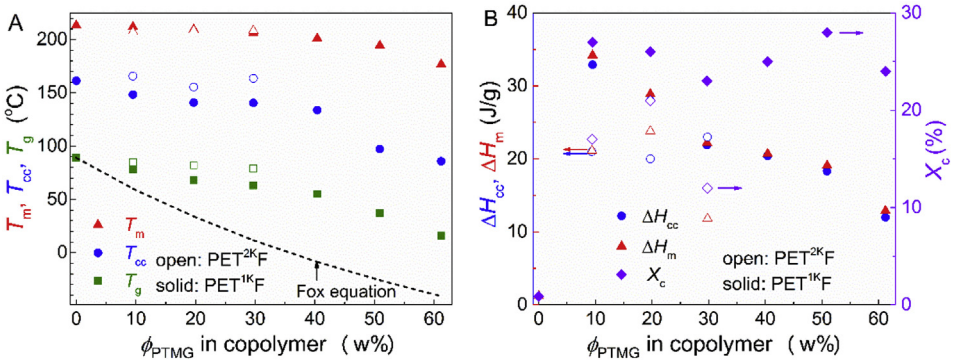

Fig. 4. Composition dependences of (A) glass transition temperature (T_g), cold crystallization temperature (T_{cc}) and melting temperature (T_m) and (B) cold crystallization enthalpy (ΔH_{cc}), melting enthalpy (ΔH_m) and crystallinity (X_c) of PEF segments in PETF copolymers. The dashed line shows the values calculated using the Fox Equation: $1/T_g = \phi_{PTMG}/T_{g,PTMG} + (1-\phi_{PTMG})/T_{g,PEF}$, $T_{g,PEF}$ = 89 °C, $T_{g,PTMG}$ = −84 °C [41].

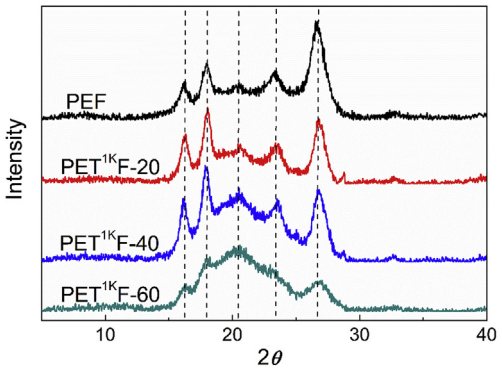

Fig. 5. WAXD patterns of PEF and PET^{1K}F copolymers.

150 °C for 3 h, which is in agreement with α′-type crystal of PEF reported by previous reports [43–45]. It can also be observed that the PET^{1K}F copolymers have almost unchanged WAXD peak locations with respect to PEF, indicating that the presence of PTMG^{1K} segments does not change the crystal structure of EF segments.

3.4. Thermal stability

Thermal stability of the PET^{1K}F copolymers was evaluated by TGA under N_2 atmosphere, taking PEF homopolymer as a reference. The TGA curves are shown in Fig. 6, the decomposition temperatures at 5% weight loss and the maximum decomposition rate ($T_{d,5}$, $T_{d,max}$) are listed in Table 1. The PEF homopolymer shows $T_{d,5}$ of 376 °C and $T_{d,max}$ of 416 °C, highlighting excellent thermal stability. Like PEF, all the PET^{1K}F copolymers show single-step thermal decomposition, but their thermal stability is clearly deteriorated because of the existence of the more susceptible ether linkage in PTMG segments. They show $T_{d,5}$ ranging 333–342 °C and $T_{d,max}$ 386–394 °C, which are almost independent of the PTMG^{1K} content and about 40 °C and 25 °C lower than those of PEF, respectively. The residual weight decreases gradually with the PTMG^{1K} content. However, the thermal decomposition does not take place before 300 °C for all the copolymers. Therefore, their thermal stability is sufficiently enough for processing them at temperature higher than their melting temperature.

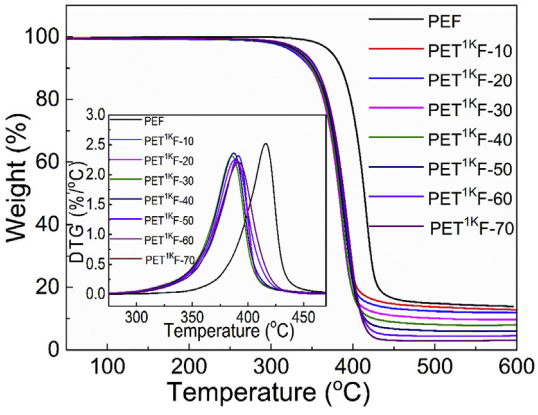

Fig. 6. TGA thermograms of PEF and PET^{1K}F copolymers under N_2 atmosphere. (heating rate: 10 °C/min).

3.5. Mechanical properties

Typical tensile stress-strain curves of PEF and PETF copolymers are shown in Fig. 7. The tensile properties including Young's modulus (E), tensile strength at yield (σ_y) and break (σ_b) and elongation at yield (ε_y) and break (ε_b) are summarized in Table 3. The composition dependences of the tensile properties are plotted in Fig. 8. The PEF samples were broken in a typical brittle fracture mode, showing very high tensile modulus (3.4 GPa) and strength (84 MPa) but very low elongation at break (3%). The rigidity and strength are among the best results previously reported [15,21,24–26]. Like PEF, PET^{1K}F-10 experienced brittle fracture too, showing almost unchanged ε_b and a slightly lower E and σ_b. Different from PET^{1K}F-10, PET^{1K}F-20 was broken in a typical ductile fracture mode, experiencing yielding/necking at ε_y of 4% then plastic deformation. PET^{1K}F-20 not only shows very high elongation at break (252%) but also retains high modulus (3.0 GPa) and yielding strength (74 MPa) though the breaking strength decreases clearly to 36 MPa. PET^{1K}F-30 exhibits similar tensile behavior like PET^{1K}F-20, but the modulus and strength further decreases. At ϕ_{PTMG} at 30 w%, there is no necking observed, but weak yielding is still observable. For PET^{1K}Fs with ϕ_{PTMG} ranging 35–60 w%, yielding/necking no longer occurred but typical rubber plateaus appeared during the tensile process. As thermoplastic elastomers, they show excellent tensile properties, with tensile modulus ranging 39–800 MPa, strength

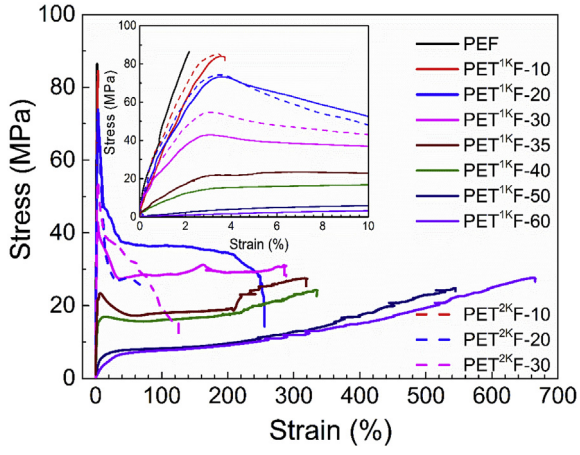

Fig. 7. Typical stress-strain curves of PEF and PETF copolymers.

Table 3
Young's modulus (E), tensile strength at yield (σ_y) and break (σ_b), elongation at yield (ε_y) and break (ε_b), notch impact strength (σ_i) and O_2 permeability coefficient (P_{O2}) of PEF and PETF copolymers.

Sample	E (GPa)	σ_y (MPa)	σ_b (MPa)	ε_y (%)	ε_b (%)	σ_i (kJ/m^2)	P_{O2} (barrer)
PEF	3.43 ± 0.16	nd	84 ± 2	nd	3 ± 1	2.1 ± 0.1	0.012
PET^{1K}F-10	3.22 ± 0.30	nd	79 ± 6	nd	4 ± 1	2.1 ± 0.1	
PET^{1K}F-20	2.99 ± 0.28	74 ± 1	36 ± 2	4 ± 1	252 ± 22	2.2 ± 0.5	0.042
PET^{1K}F-30	1.83 ± 0.38	40 ± 2	29 ± 3	3 ± 1	258 ± 26	6.4 ± 0.5	
PET^{1K}F-35	0.80 ± 0.15	–	26 ± 1	nd	272 ± 34	52.6 ± 2	
PET^{1K}F-40	0.54 ± 0.19	–	24 ± 2	nd	318 ± 45	58.8 ± 5	0.28
PET^{1K}F-50	0.092 ± 0.015	–	22 ± 3	nd	534 ± 38	nd	
PET^{1K}F-60	0.039 ± 0.003	–	25 ± 2	nd	684 ± 32	nd	1.77
PET^{2K}F-10	3.41 ± 0.62	–	83 ± 6	nd	3 ± 1	2.1 ± 0.1	
PET^{2K}F-20	3.10 ± 0.34	76 ± 1	33 ± 6	4 ± 1	71 ± 36	2.2 ± 0.1	
PET^{2K}F-30	2.18 ± 0.21	52 ± 2	12 ± 3	3 ± 1	104 ± 39	4.1 ± 0.6	

ranging 22–26 MPa, and high elongation at break ranging 272–684%. Among them, PET^{1K}F-60 has higher tensile strength than PET^{1K}F-50 (25 vs. 22 MPa) because of its higher intrinsic viscosity (see Table 1). At higher ϕ_{PTMG}, the copolymers have too low T_g (lower than room temperature) to be able to satisfy the requirements for specimen preparation and tensile test.

In comparison with the PET^{1K}Fs, the PET^{2K}Fs exhibited similar tensile behaviors at the same composition range 10–30 w%, but experienced clear "stress-softening" after yielding/necking at ϕ_{PTMG} of 20–30%. PET^{2K}F-20 and PET^{2K}F-30 show higher tensile modulus (3.1–2.2 GPa vs. 3.0–1.8 GPa), yielding strength (76-52 MPa vs. 74-40 MPa), but clearly lower breaking strength (33-12 MPa vs. 36-29 MPa) and elongation at break (71–104% vs. 252–258%). These results indicate that PTMG^{2K} is also able to toughen PEF at ϕ_{PTMG} over 20%, but the effect is inferior to PTMG^{1K}. The differences in tensile properties are ascribed to the existence of PTMG^{2K} crystals in PET^{2K}Fs, in contrast, amorphous and more miscible PTMG^{1K} segments in PET^{1K}Fs. With low T_m (~26 °C) equal to room temperature, the PTMG^{2K} crystals might fuse during tensile testing because of thermogenesis caused by chain stretching, which could be responsible for the observed "stress-softening". Therefore, the molecular weight of PTMG flexible segment should be selected with care in designing PETF multiblock copolymers.

Impact toughness of the PETF copolymers was further examined through notched Izod impact test. The impact strength (σ_i) are listed in Table 3 and shown in Fig. 8D. Although clear brittle-ductile transition occurs and high tensile toughness or ductility is obtained in tensile test at 20 w% ϕ_{PTMG}, the impact strength is not improved until the ϕ_{PTMG} reaches 30 w%. PET^{1K}F-30 and PET^{2K}F-30 show impact strength of 6.4 ± 0.5 and 4.1 ± 0.6 kJ/m^2, respectively. The improvement factor of impact strength defined by $\sigma_i/\sigma_{i,PEF}$ are 3 and 2 folds, respectively. For the same reason mentioned above, PTMG^{1K} shows better toughening effect than PTMG^{2K}. The impact strengths of these two samples are average values of ten specimens for each sample. Five specimens were measured on one testing machine and the others on another machine. The two independent measurements gave reproducible results. At ϕ_{PTMG} of 35–40 w%, the impact strength of PET^{1K}F-35 and PET^{1K}F-40 are as high as 52.6 and 58.8 kJ/m^2, being 24 and 27 times higher than the value measured for PEF, respectively. From Fig. 8D, it can be seen that the brittle-tough transition locates at ϕ_{PTMG} between 30 w% and 35 w%. PET^{1K}F-50 and PET^{1K}F-60 are typical thermoplastic elastomers and therefore cannot be ruptured during the impact test.

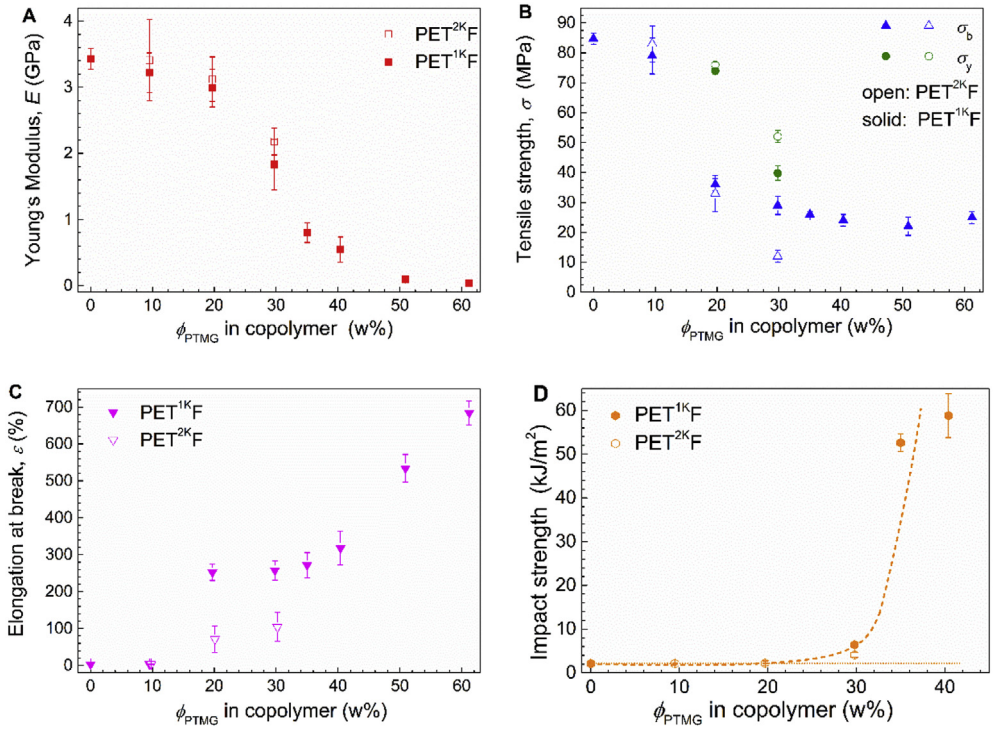

Fig. 8. Composition dependences of tensile and impact properties of PETF copolymers.

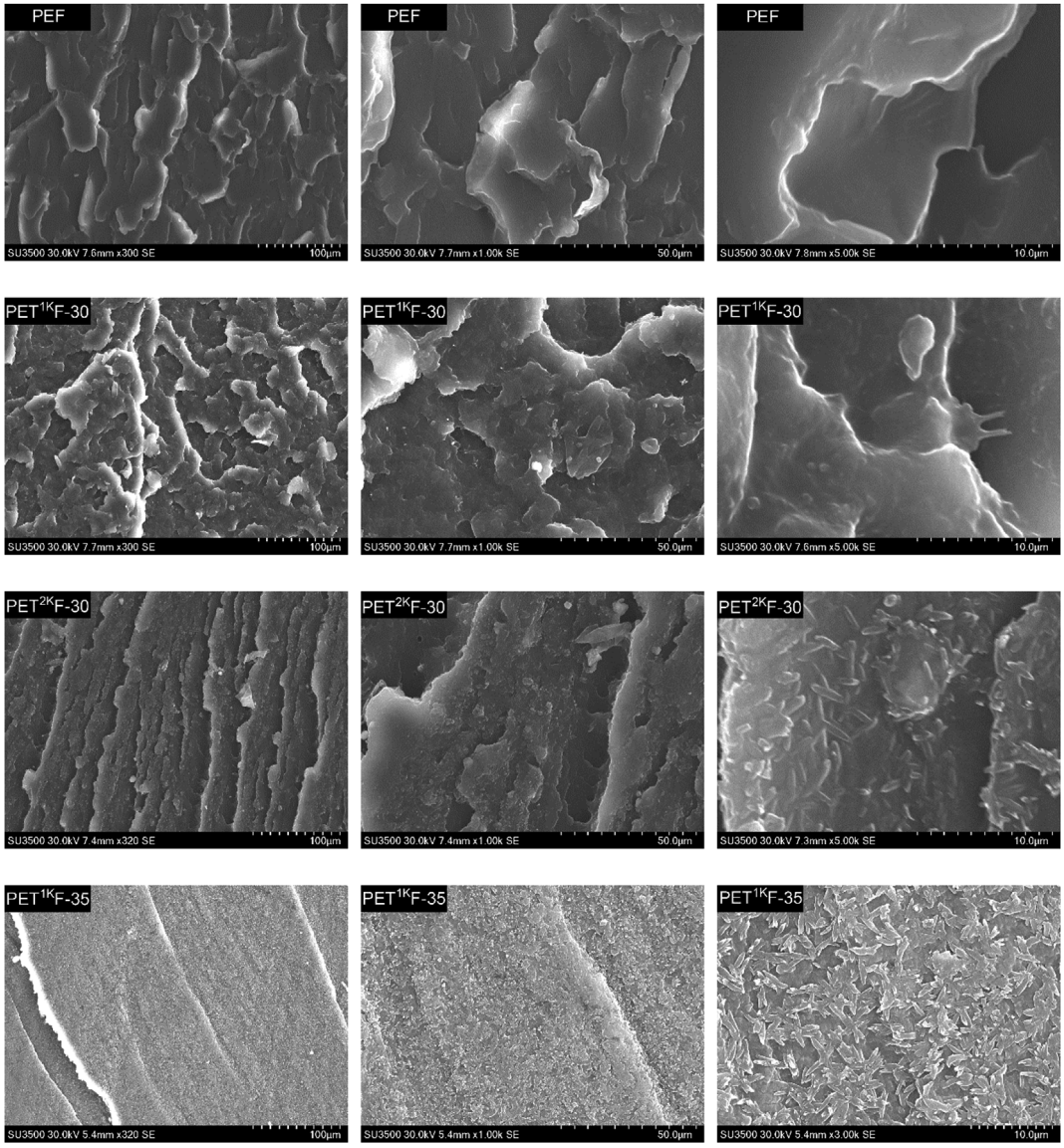

Fig. 9. Impact fracture surface morphology of PEF, $PET^{1K}F$-30, $PET^{2K}F$-30 and $PET^{1K}F$-35.

PEF is a brittle polymer, even at high molecular weight. Some random and multiblock copolymers of PEF have been reported to improve its mechanical properties including toughness. In comparison with copolymers containing flexible components like P(EF-mb-PEG) [26], poly(ethylene sebacate-co-furandicarboxylate) [24], the PETF multiblock copolymers in this study show not only higher ductility but also higher strength and modulus. The strength and modulus at ϕ_{PTMG} of 10–30 w% are even comparable to some random copolymers containing rigid components, including poly(ethylene terephthalate-co-furandicarboxylate) [27], poly(ethylene-co-1,4-cyclohexanedimethylene furandicarboxylate) (PECF) [21] and poly(ethylene-co-2,2,4,4-tetramethyl-1,3-cyclobutanediol furandicarboxylate) [25]. With respect to improving impact toughness of PEF, Park et al. reported the first and sole result to date [20]. They synthesized PECF and found that the notched Izod impact strength was slightly improved from 3.1 kg cm/cm of PEF to 4.0 kg cm/cm of $PE_{25}C_{75}F$. The improvement factor is only of 1.3. Our study also indicates it is not easy to improve impact toughness of PEF. It needs more PTMG to reach brittle-tough transition in impact testing than to reach brittle-ductile transition in tensile testing. But clearly, higher impact toughness has been achieved in the PETF copolymers.

Therefore, the mechanical properties of PETF copolymers can be tailor-made from high performance toughened thermoplastics to thermoplastic elastomers through changing the content of $PTMG^{1K}$ segments. Among them, $PET^{1K}F$-20 has excellent tensile properties and high enough T_g comparable to bottle grade PET. If high impact toughness is required, $PET^{1K}F$-30 or $PET^{1K}F$-35 are better choices. In conclusion, the PETF copolymers appear to be promising materials for practical applications.

3.6. Fracture morphology

Finally, the impact fracture surface morphology of PEF, $PET^{1K}F$-30, $PET^{2K}F$-30 and $PET^{1K}F$-35 was observed with SEM to help understanding the toughening mechanism. As shown in Fig. 9, spherical and strip-like PTMG particles with size from 0.5 to several microns can be observed on the fracture surface of the multiblock copolymers, particularly $PET^{2K}F$-30 and $PET^{1K}F$-35, suggesting that phase separation occurred. PEF shows a smooth fracture surface resulting from brittle fracture. In comparison, both $PET^{1K}F$-30 and $PET^{2K}F$-30 exhibit coarse fracture surface, more likely as a result of the enhanced toughness as previously recorded by mechanical testing. While the plasticization effect of $PTMG^{1K}$ segments on the resulting multiblock copolymers likely contributes to the toughening effect at least at lower soft segment

content (ϕ_{PTMG} 10–30 w%), the strip-like PTMG particles observed for PET^{1K}F-35 may account for its super toughness. It can be seen from Fig. 8D that the brittle-tough transition of PET^{1K}F occurs before ϕ_{PTMG} reaches 35 w%, indicating the average inter-particle distance is less than the critical value for brittle-tough transition. Acting as stress centers, the dense PTMG^{1K} particles in PET^{1K}F-35 not only initiates crazing and shear zone, but also inhibits and terminate propagation of crazing. They can also bridge and branch crazing, which is more beneficial to the dissipation of impact energy.

3.7. Oxygen barrier property

The O_2 permeability coefficient (P_{O2}) of PEF, PET^{1K}F-20, PET^{1K}F-40 and PET^{1K}F-60 measured at 23 °C and 50 RH% are listed in Table 3 too. The P_{O2} value of PEF is as high as 0.012 barrer in this work. It agrees well with the results reported by Burgess et al. (0.0107 barrer) [16] and Wang et al. (0.011 barrer) [21]. It has been reported that the high O_2 barrier performance of PEF comes from the restricted chain mobility caused by the hindrance of furan ring flipping [28]. However, the P_{O2} value of the PET^{1K}F copolymers increases with increasing PTMG content. The P_{O2} value of PET^{1K}F-20 is 0.042 barrer, still being lower than the results of PET reported by Burgess et al. (0.114 barrer) [16] and Wang et al. (0.06 barrer) [21]. But the P_{O2} value of PET^{1K}F-40 and PET^{1K}F-60 dramatically increases to 0.28 barrer and 1.77 barrer respectively, which are close to the results of PBAT (0.94 barrer) [46] and PP (1.2 barrer) [47] respectively. The results indicate that incorporating PTMG into PEF significantly weakens the O_2 barrier performance of the resulting materials, possibly due to the superior chain flexibility and mobility of PTMG segment. New PEF copolymers with high gas barrier performance as well as balanced mechanical properties will be reported soon.

4. Conclusions

P(EF-mb-PTMG) (or PETF, for simplicity) multiblock copolymers with high intrinsic viscosity were successfully synthesized via melt polycondensation of DMFD and EG in the presence of PTMG^{1K} and PTMG^{2K} oligomer diols, characterized with FTIR, ^{1}H NMR, DSC, WAXD, TGA and SEM, and assessed with tensile and impact testing. The presence of PTMG not only promotes intrinsic viscosity growth but also depresses DEGF unit formation during polycondensation, and the feeding ratio of PTMG controls the copolymer composition quite well. The PTMG^{1K} flexible segments show chain length dependent partial miscibility with PEF hard segments, being less miscible for PTMG^{2K}. Therefore, the presence of PTMG segments results in plasticization and cold crystallizability promotion of PEF segments, keeping PEF crystal structure unchanged. Through incorporating PTMG, PEF-based high performance materials from toughened thermoplastics with excellent ductility and impact toughness to thermoplastic elastomers with high strength have been successfully obtained. Among them, PET^{1K}F-20 shows excellent ductility (elongation at break as high as 252%) and retains high modulus (3.0 GPa) and yielding strength (74 MPa) at the same time, and PET^{1K}F-35 is the first PEF-based material with impact strength over 50 kJ/m^2 to date. Possessing tunable and superior mechanical properties, excellent thermal stability and high enough T_g, these copolymers seem to have promising prospects for practical applications in thermoplastics, elastomers and toughening modifiers.

Acknowledgements

This work was supported by the National Natural Science Foundation of China (51773177), State Key Laboratory of Chemical Engineering (No. SKL-ChE-18D02), the National Key Research and Development Program (2016YFB0302402) and 151 Talents Project of Zhejiang Province. The authors are also very grateful to Shuangling Luo from Ningbo Institute of Technology, Zhejiang University, for her kind help in term of oxygen permeability test.

Appendix A. Supplementary data

Supplementary data to this article can be found online at https://doi.org/10.1016/j.polymer.2018.09.033.

References

[1] J.J. Bozell, Feedstocks for the future-biorefinery production of chemicals from renewable carbon, Clean. - Soil, Air, Water 36 (2008) 641–647.
[2] B.J. Nikolau, M.A.D.N. Perera, L. Brachova, B. Shanks, Platform biochemicals for a biorenewable chemical industry, Plant J. 54 (2008) 536–545.
[3] A. Gandini, Polymers from renewable resources: a challenge for the future of macromolecular materials, Macromolecules 41 (2008) 9491–9504.
[4] J. Coombs, K. Hall, Chemicals and polymers from biomass, Renew. Energ. 15 (1998) 54–59.
[5] U.T. Bornscheuer, Feeding on plastic, Science 351 (2016) 1154–1155.
[6] T. Fecker, P. Galaz-Davison, F. Engelberger, Y. Narui, M. Sotomayor, L.P. Parra, Active site flexibility as a hallmark for efficient PET degradation by I. Sakaiensis PETase, Biophys. J. 114 (2018) 1302–1312.
[7] A. Llevot, E. Grau, S. Carlotti, S. Grelier, H. Cramail, From lignin-derived aromatic compounds to novel biobased polymers, Macromol. Rapid Commun. 37 (2016) 9–28.
[8] S.B. Peng, L.B. Wu, B.G. Li, P. Dubois, Hydrolytic and compost degradation of biobased PBSF and PBAF copolyesters with 40–60mol% BF unit, Polym. Degrad. Stab. 146 (2017) 223–228.
[9] S.B. Peng, Z.Y. Bu, L.B. Wu, B.G. Li, P. Dubois, High molecular weight poly(butylene succinate-co-furandicarboxylate) with 10 mol% of BF unit: synthesis, crystallization-melting behavior and mechanical properties, Eur. Polym. J. 96 (2017) 248–255.
[10] J.P. Wu, H.Z. Xie, L.B. Wu, B.G. Li, P. Dubois, DBU-catalyzed biobased poly(ethylene 2,5-furandicarboxylate) polyester with rapid melt crystallization: synthesis, crystallization kinetics and melting behavior, RSC Adv. 6 (2016) 101578–101586.
[11] V. Tsanaktsis, Z. Terzopoulou, M. Nerantzaki, G.Z. Papageorgiou, D.N. Bikiaris, New poly(pentylene furanoate) and poly(heptylene furanoate) sustainable polyesters from diols with odd methylene groups, Mater. Lett. 178 (2016) 64–67.
[12] V. Tsanaktsis, Z. Terzopoulou, S. Exarhopoulos, D.N. Bikiaris, D.S. Achilias, D.G. Papageorgiou, G.Z. Papageorgiou, Sustainable, eco-friendly polyesters synthesized from renewable resources: preparation and thermal characteristics of poly (dimethyl-propylene furanoate), Polym. Chem. 6 (2015) 8284–8296.
[13] V. Tsanaktsis, G.Z. Papageorgiou, D.N. Bikiaris, A facile method to synthesize high-molecular-weight biobased polyesters from 2,5-furandicarboxylic acid and long-chain diols, J. Polym. Sci. Part A Polym. Chem. 53 (2015) 2617–2632.
[14] L.B. Wu, R. Mincheva, Y.T. Xu, J.M. Raquez, P. Dubois, High molecular weight poly (butylene succinate-co-butylene furandicarboxylate) copolyesters: from catalyzed polycondensation reaction to thermomechanical properties, Biomacromolecules 13 (2012) 2973–2981.
[15] M. Jiang, Q. Liu, Q. Zhang, C. Ye, G.Y. Zhou, A series of furan-aromatic polyesters synthesized via direct esterification method based on renewable resources, J. Polym. Sci. Part A Polym. Chem. 50 (2012) 1026–1036.
[16] S.K. Burgess, O. Karvan, J.R. Johnson, R.M. Kriegel, W.J. Koros, Oxygen sorption and transport in amorphous poly(ethylene furanoate), Polymer 55 (2014) 4748–4756.
[17] S.K. Burgess, R.M. Kriegel, W.J. Koros, Carbon dioxide sorption and transport in amorphous poly(ethylene furanoate), Macromolecules 48 (2015) 2184–2193.
[18] A.J.J.E. Eerhart, A.P.C. Faaij, M.K. Patel, Replacing fossil based PET with biobased PEF; process analysis, energy and GHG balance, Energy Environ. Sci. 5 (2012) 6407–6422.
[19] A. Codou, N. Guigo, J.V. Berkel, E.D. Jong, N. Sbirrazzuoli, Non-isothermal crystallization kinetics of biobased poly(ethylene 2,5-furandicarboxylate) synthesized via the direct esterification process, Macromol. Chem. Phys. 215 (2015) 2065–2074.
[20] S. Hong, O.O. Park, High molecular weight bio furan-based co-polyesters for food packaging applications, Green Chem. 18 (2016) 5142–5150.
[21] J.G. Wang, X.Q. Liu, Y.J. Zhang, F. Liu, J. Zhu, Modification of poly(ethylene 2,5-furandicarboxylate) with 1,4-cyclohexanedimethylene: influence of composition on mechanical and barrier properties, Polymer 103 (2016) 1–8.
[22] R.J.I. Knoop, W. Vogelzang, J.V. Haveren, D.S. van Es, High molecular weight poly (ethylene-2,5-furanoate); critical aspects in synthesis and mechanical property determination, J. Polym. Sci. Part A Polym. Chem. 51 (2013) 1026–1036.
[23] G.Z. Papageorgiou, D.G. Papageorgiou, Z. Terzopoulou, D.N. Bikiaris, Production of bio-based 2,5-furan dicarboxylate polyesters: recent progress and critical aspects in their synthesis and thermal properties, Eur. Polym. J. 83 (2016) 202–229.
[24] G.Q. Wang, M. Jiang, Q. Zhang, R. Wang, G.Y. Zhou, Biobased copolyesters: synthesis, crystallization behavior, thermal and mechanical properties of poly (ethylene glycol sebacate-co-ethylene glycol 2,5-furan dicarboxylate), RSC Adv. 7 (2017) 13798–13807.
[25] J.G. Wang, X.Q. Liu, J. Zhen, Y. Liu, L.Y. Sun, J. Zhu, Synthesis of bio-based poly (ethylene 2,5-furandicarboxylate) copolyesters: higher glass transition temperature, better transparency, and good barrier properties, J. Polym. Sci. Part A Polym. Chem. 55 (2017) 3298–3307.
[26] G.Q. Wang, M. Jiang, Q. Zhang, R. Wang, G.Y. Zhou, Biobased multiblock

copolymers: synthesis, properties and shape memory performance of poly(ethylene2,5-furandicarboxylate)-b-poly(ethylene glycol), Polym. Degrad. Stab. 144 (2017) 121–127.
[27] M. Jiang, T.T. Lu, G.W. Jiang, Q. Zhang, G.Y. Zhou, Acta Polym. Sin. 46 (2013) 1092–1098.
[28] S.K. Burgess, J.E. Leisen, B.E. Kraftschik, C.R. Mubarak, R.M. Kriegel, W.J. Koros, Chain mobility, thermal, and mechanical properties of poly(ethylene furanoate) compared to poly(ethylene terephthalate), Macromolecules 47 (2014) 1383–1391.
[29] D.S. Achilias, A. Chondroyiannis, M. Nerantzaki, K.V. Adam, Z. Terzopoulou, G.Z. Papageorgiou, D.N. Bikiaris, Solid state polymerization of poly(ethylene furanoate) and its nanocomposites with SiO_2 and TiO_2, Macromol. Mater. Eng. 302 (2017) 1700012.
[30] N. Lotti, A. Munari, M. Gigli, M. Gazzano, V. Tsanaktsis, D.N. Bikiaris, G.Z. Papageorgiou, Thermal and structural response of in situ prepared biobased poly(ethylene 2,5-furan dicarboxylate) nanocomposites, Polymer 103 (2016) 288–298.
[31] A. Codou, N. Guigo, J.G. van Berkel, J.E. De, N. Sbirrazzuoli, Preparation and crystallization behavior of poly(ethylene 2,5-furandicarboxylate)/cellulose composites by twin screw extrusion, Carbohyd. Polym. 174 (2017) 1026–1033.
[32] A. Codou, N. Guigo, J.G. van Berkel, J.E. De, N. Sbirrazzuoli, Preparation and characterization of poly(ethylene 2,5-furandicarboxylate/nanocrystalline cellulose composites via solvent casting, J. Polym. Eng. 37 (2017) 869–878.
[33] L. Martino, N. Guigo, J.G.V. Berkel, N. Sbirrazzuoli, Influence of organically modified montmorillonite and sepiolite clayson the physical properties of bio-based poly (ethylene 2,5-furandicarboxylate), Compos. B Eng. 110 (2017) 96–105.
[34] M. Konstantopoulou, Z. Terzopoulou, M. Nerantzaki, J. Tsagkalias, D.S. Achilias, D.N. Bikiaris, S. Exarhopoulos, D.G. Papageorgiou, G.Z. Papageorgiou, Poly(ethylene furanoate-co-ethylene terephthalate) biobased copolymers: synthesis, thermal properties and cocrystallization behavior, Eur. Polym. J. 89 (2017) 349–366.
[35] Z. Terzopoulou, V. Tsanaktsis, D.N. Bikiaris, S. Exarhopoulos, D.G. Papageorgiou, G.Z. Papageorgiou, Biobased poly(ethylene furanoate-co-ethylene succinate) copolyesters: solid state structure, melting point depression and biodegradability, RSC Adv. 6 (2016) 84003–84015.
[36] M. Matos, A.F. Sousa, A.J.D. Silvestre, Improving the thermal properties of poly (2,5-furandicarboxylate)s using cyclohexylene moieties: a comparative study, Macromol. Chem. Phys. 218 (2016) 1600492.
[37] J.P. Ma, Y. Pang, M. Wang, J. Xu, H. Ma, X. Nie, The copolymerization reactivity of diols with 2,5-furandicarboxylic acid for furan-based copolyester materials, J. Mater. Chem. 22 (2012) 3457–3461.
[38] J.W. Zhang, F. Liu, J.G. Wang, H.N. Na, J. Zhu, Synthesis of Poly(butylene terephthalate)-poly(tetramethylene glycol) copolymers using terephthalic acid as starting material: a comparation between two synthetic strategies, Chin. J. Polym. Sci. 33 (2015) 1283–1293.
[39] F. Liu, J. Zhang, J. Wang, H.N. Na, J. Zhu, Incorporation of 1,4-cyclohexanedicarboxylic acid into poly(butylene terephthalate)-b-poly(tetramethylene glycol) to alter thermal properties without compromising tensile and elastic properties, RSC Adv. 5 (2015) 94091–94098.
[40] W.D. Zhou, Y.J. Zhang, Y. Xu, P.L. Wang, L. Gao, W. Zhang, J. Ji, Synthesis and characterization of bio-based poly(butylene furandicarboxylate)-b-poly(tetramethylene glycol) copolymers, Polym. Degrad. Stab. 109 (2014) 21–26.
[41] E.B. Mark, Polymer Data Handbook, Oxford University, 1999.
[42] E.B. Brandrup, I.H. Immergut, E.A. Grulke, Polymer Handbook, John Wiley & Sons, 1999.
[43] G. Stoclet, G.G.D. Sart, B. Yeniad, S.D. Vos, J.M. Lefebvre, Isothermal crystallization and structural characterization of poly(ethylene 2,5-furanoate), Polymer 72 (2015) 165–176.
[44] V. Tsanaktsis, D.G. Papageorgiou, S. Exarhopoulos, D.N. Bikiaris, G.Z. Papageorgiou, On the crystallization and polymorphism of poly(ethylene furanoate), Cryst. Growth Des. 15 (2015) 5505–5512.
[45] L. Maini, M. Gigli, M. Gazzano, N. Lotti, D.N. Bikiaris, G.Z. Papageorgiou, Structural investigation of poly(ethylene furanoate) polymorphs, Polymers 10 (2018) 296.
[46] P.G. Ren, X.H. Liu, F. Ren, G.J. Zhong, X. Ju, L. Xu, Biodegradable graphene oxide nanosheets/poly-(butylene adipate-co-terephthlate) nanocomposite film with enhanced gas and water vapor barrier properties, Polym. Test. 58 (2017) 173–180.
[47] N. Inagaki, S. Tasaka, T. Nakajima, Preparation of oxygen gas barrier polypropylene films by deposition of SiOx film plasma-polymerized from mixture of tetramethoxysilane and oxygen, J. Appl. Polym. Sci. 78 (2000) 2389–2397.